Water Resources and Industry 6 (2014) 1–17

Contents lists available at ScienceDirect

Water Resources and Industry

journal homepage: www.elsevier.com/locate/wri

Kinetic, equilibrium and thermodynamic investigations of Ni(II), Cd(II), Cu(II) and Co(II) adsorption on barley straw ash

M. Arshadi [a,*], M.J. Amiri [b], S. Mousavi [c]

[a] Department of Science, Fasa Branch, Islamic Azad University, PO Box 364, Fasa 7461713591, Fars, Iran
[b] Department of Water Engineering, College of Agriculture, Fasa University, 74617-81189 Fasa, Iran
[c] Department of Chemistry, Malek-ashtar University of Technology, P.O. Box 83145/115, Shahin-Shahr, Iran

ARTICLE INFO

Article history:
Received 28 April 2014
Received in revised form
7 June 2014
Accepted 12 June 2014

Keywords:
Bioadsorbent
Heavy metal
Adsorption
Ash
Barley straw

ABSTRACT

This work reports the application of a straw ash from barley as a novel bioadsorbent for the removal of several heavy metals: Ni(II), Cd(II), Cu(II), and Co(II). Equilibrium and kinetic models for heavy metals sorption were developed by considering the effect of the contact time, initial heavy metal ion concentrations, effect of temperature, and initial pH. The adsorption of heavy metal ions have been studied in terms of pseudo-first- and -second-order kinetics, and the Freundlich, Langmuir and Langmuir–Freundlich isotherms models have also been used to the equilibrium adsorption data. The equilibrium data fitted well with the Langmuir–Freundlich model and showed the following affinity order of the material: Ni(II) > Cu(II) > Co(II) > Cd(II). The adsorption kinetics followed the mechanism of the pseudo-second-order equation for all systems studied, confirming chemical sorption as the rate-limiting step of adsorption mechanisms. The thermodynamic parameters (ΔG°, ΔH° and ΔS°) indicated that the adsorption of heavy metals ions were feasible, spontaneous and endothermic at 15–80 °C.

* Corresponding author. Tel.: +98 9361528179.
E-mail addresses: m-arshadi@ch.iut.ac.ir, mohammadarshadi@yahoo.com (M. Arshadi).

http://dx.doi.org/10.1016/j.wri.2014.06.001

1. Introduction

Agriculture is a source of energy through its production of biomass, which can be used as biofuel and is a renewable resource [1]. An interest in contribution of biomass to the energy supply received considerable attention during the 1970s because of the urgency of obtaining energy self-sufficiency [2,3] which has been renewed since the mid-1990s because of the quest for mitigating global climate change [4]. Recently, one of the current interests in the world is to investigate whether cereals and crop residues could be an alternative energy source to fossil fuels [5]. The identification of cereal species and varieties with high biomass yield, high combustibility, low ash content, and low potential for boiler corrosion is a priority. Annual crops such as wheat, rye, or triticale, cultivated as an alternative energy source, do not require high investment, and they are easy to rotate in the crop cycle. Cultivation, fertilization, and harvesting techniques are essential to ensure the optimal use of resources.

Because of the toxicity of heavy metals, the Agency for Toxic Substances and Disease Registry, of the U.S. Department of Health and Human Services, has designated these chemicals as priority pollutants [6]. However, Cd, Cu, Ni and Co are considered the most hazardous and are included on the US Environmental Protection Agency's (EPA) list of priority pollutants [7]. Cd, Cu, Ni and Co are highly toxic substances, exposure to which can produce a wide range of adverse health effects for both adults and children at very low levels [6]. The inorganic pollutions considered in this paper, are the widely used elements, where an intake of excessively large doses by man may lead to serious kidney failure and liver disease [6]. In fact, industrial activity has caused widespread pollution of soil by elements such as Pb, Cd, Cu, Hg, Co, Zn, and also Ni [7–9].

The following conventional methods used in heavy metals removal from wastewater: coagulation and flocculation, oxidation or ozonation, membrane separation, and adsorption [9]. Adsorption processes have been reported to be the low-cost promising alternatives for the treatment of heavy metals present in wastewater. Most of these methods suffer from drawbacks like high capital and operational costs and there are problems in disposal of the residual metal sludge [10]. Activated carbon is the most prevailing adsorbent for this process because of its high surface area, high adsorption capacity, and high degree of surface reactivity; however, it is expensive and must be regenerated on a regular basis. Accordingly, improved and innovative methods for water and wastewater treatment are continuously being developed to treat water-containing metals. However, biomaterial supports present several advantages with respect to activated carbon, including better mechanical stability and a higher concentration of chelating groups on the surface, and they are often much cheaper than the synthesized organic and inorganic supports. Seaweed [11], mushroom harvest residues [12], pine bark, pine needles and leaves [13], modified chitosan, cassava, and loofah sponge [12], and saw dust [14,15] have been used as potential adsorbents in research studies.

Producing and using biomass requires other inputs such as diesel oil, nitrogen fertilizer, and pesticides which, depending on the type, dosage, and utilization, have a negative impact on the environment compared to that of fallow fields. Economic estimations show that energy crops have high potential, so they form a major element in the long-term world energy strategy [1]. The challenge for research programs is to find the most cost effective and least damaging way to use this resource. If we accept that biomass can be seen in the long term as a universal sustainable replacement for fossil raw materials once the extensive research and development work has been completed and if future in the world decide to use the energy of crops, ashes from combustion of biofuels should be regarded also as a resource. Therefore, the data presented in this study could be helpful with regard to the usefulness of the ash as nonconventional adsorbent for the removal of pollutants. In Iran barley is one of the major cereal crops grown on the prairies. The agricultural by-product represents a potential alternative as an anion exchanger because of its particular properties such as its chemical stability and high reactivity, resulting from the presence of reactive hydroxyl groups in polymer chains. However, the barley straw was found to show poor efficiency for heavy metals removal. This was expected as raw agricultural waste usually showed low sorption capacity and, thus, pretreatment of the raw material seems necessary to raise its efficiency [16]. The aim of this research is to evaluate the performance and effectiveness of barley straw ash (BSA) as a novel bioadsorbent for the removal of four inorganic contaminants that present in typical wastewater: Ni(II), Cd(II), Cu(II), and Co(II). The influences of environmental factors (initial pH value, reaction time, initial heavy metal ions

concentration, temperature effect.) that affect adsorption were compared. Furthermore, the adsorption of heavy metal ions has been studied in terms of pseudo-first-order and pseudo-second-order kinetics, and the Langmuir, Freundlich and Langmuir–Freundlich adsorption isotherm equations are applied to the experimental data to obtain information about the interaction between the inorganic pollutants and the cereal ash.

2. Experimental

2.1. Materials and analytical techniques

All reagents (AR grade) were purchased from Merck or Fluka and used without further purification, except for solvents, which were treated according to standard methods. Stock solutions of Cd, Ni, Co, and Cu were prepared from analytical grade chemicals, $Cd(NO_3)_2$, $Ni(NO_3)_2$, $Co(NO_3)_2$ and $Cu(NO_3)_2$. Solution of 0.1 M NaOH and 0.1 M HNO_3 were used for pH adjustment by a pH meter (Metrohm, 827 pH Lab). All working solutions were prepared by diluting the stock solutions with deionized water. The concentrations of heavy metal ion solutions were measured by atomic absorption spectrophotometry using a Perkin-Elmer 3030 instrument. Infrared was collected on KBr pellets using a JASCO FT/IR (680 plus) spectrometer. Chemical analyses are carried out by inductively coupled plasma atomic emission spectroscopy (ICP-AES, Perkin-Elmer) (spectro-flamed; typically, 30 mg sample was dissolved in 500 μl 40% HF solution, 4 mL 1:4 HCl:H_2SO_4 solution and 45 mL H_2O). The specific surface areas were calculated using the BET method and the total pore volume from the nitrogen adsorbed at a relative pressure of 0.95. The pore size was calculated using the Barrett–Joyner–Halenda (BJH) method. SEM analysis (SEM-Seron, AIS2100) was used to examine the morphology and composition of the adsorbents.

2.2. Preparation of barley straw ash

The biomaterial used in the present study is obtained from cereal straw, barley straw, by the following procedure: the cereal straw is subjected to heating for 6 h at about 150 °C and then kept in a furnace for 24 h in air at 550 °C. The fraction of particle between 15 and 45 μm was selected. The solid thus obtained is stored in a vacuum desiccator until required.

2.3. Adsorption measurements

Different metals ion concentrations were freshly prepared in a solution of deionized water. Sorption experiments were carried out in batch conditions: 0.15 g of biomaterial was shaken up with a 30 mL of the inorganic pollutant, at concentrations of between 0.5 and 16 mg/L, at a controlled temperature box 25 °C. The equilibrium adsorption capacity of heavy metals onto the bioadsorbent, barley straw ash, were studied at different range of temperatures of (15, 25, 50 and 80 °C) in pH = 6.5. The time required to reach equilibrium conditions was determined by preliminary kinetic measurements. The hydrolytic stability was tested by treating nickel- and copper-loaded BSA in water at 70 °C for 24 h. To regenerate the used bioadsorbent, the metal-loaded BSA was washed with conc. HCl, resulting in complete removal of the loaded metal. After centrifugation at 3000 rpm for 15 min, the liquid phase was separated and the solute concentration determined by atomic absorption spectrophotometry.

The amount adsorbed (q_e) was calculated from the formula:

$$q_e = V \times (C_0 - C_e)/\, m \tag{1}$$

where C_0 and C_e are the initial and equilibrium liquid-phase concentrations (mg/L) of adsorbates; V is the volume of the solution (L); and m is the amount of adsorbent (g). This equation assumes that the change in volume of the bulk liquid phase is negligible as the solute concentration is small and the volume occupied by the adsorbent is also small. The amount of heavy metals adsorbed on the sample was calculated using a previously determined calibration curve. Duplicates, blanks, and reference

standards were used to obtain accurate and precise analytical data. The relative standard deviations of the analytical data were measured to less than 3.8%. The flask was immersed in an oil bath in order to make the working temperature constant at 80 °C for a predetermined time (24 h) with continuous stirring. The small aliquots of samples were withdrawn from the reaction

3. Results and discussion

The adsorption capacities for the target heavy metal ions were measured in the aqueous solution to assess the surface reactivity of the BSA. The heavy metals chosen for the investigation in single component studied were Co(II), Cu(II), Ni(II), and Cd(II).

3.1. Characterization of the barley straw ash

The image obtained by SEM of the BSA is shown in Fig. 1. It is clear from this figure that ash of barley straw has regular structure after calcination. The surface area of the BSA is rather low (3.3 m^2/g). This value can be justified by open porous structure, as it is observed in Fig. 1.

The ash of barley straw is characterized by its high percentage of K, Mg, and P, present on the hydrous oxide surface, that are responsible for metal ion binding through ion exchange mechanism

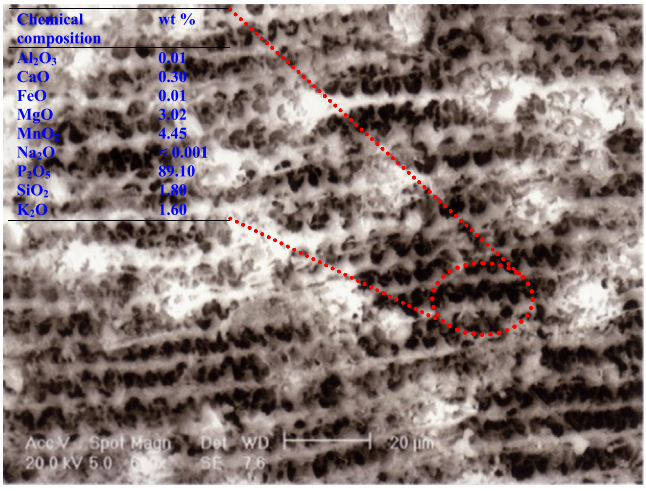

Fig. 1. SEM micrograph of barley straw ash. Inset: The chemical composition (wt%) of BSA determined by ICP-AES analysis.

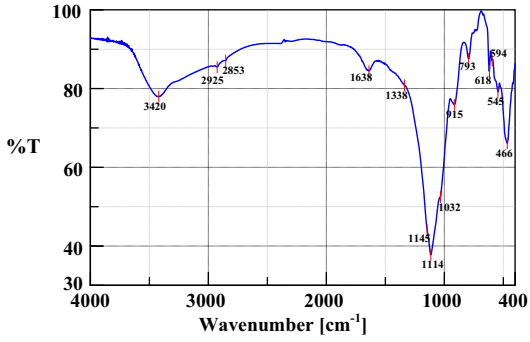

Fig. 2. FT-IR spectrum of BSA in the region 4000–400 cm^{-1}.

(Inset of Fig. 1). In addition, the ash contains a number of elements that are beneficial to plants in small doses, i.e., micronutrients, but also generally contains small amounts of undesirable heavy metals.

Inspection of infrared wave numbers (cm^{-1}) of significant valence vibrations of the BSA is collected in Fig. 2. In IR, mainly strong split phosphate (PO_4^{3-}) bands are observed in the range 1150–900 cm^{-1} (stretching mode) and 500–600 cm^{-1}. As can be seen from Fig. 2, the characteristic vibration peaks of O–P–O bonds of the phosphate appeared in the bioadsorbent as follow: 1145 cm^{-1} (HPO_4^{-2} group, P–O–H in-plane and out-of-plane deformation modes), 1338 cm^{-1} (phosphoryl (P=O) frequency), 1032 and 1114 cm^{-1} (ν_3, P–O asymmetric stretching vibrations), 915 cm^{-1} (P–OH stretching vibrations), 594 cm^{-1} (ν_4, P–O stretch), and 545 cm^{-1} (ν_4, P–O stretch and P–O bending) [17–20]. However, the BSA shows the characteristic absorption bands of symmetric and asymmetric stretching vibration of the CH_2 and CH_3 at around 2925, 2853 and 1490–1450 cm^{-1}. The strong broad band at 3420 cm^{-1} and the sharp band at 1638 cm^{-1} corresponds to the surface-adsorbed water and hydroxyl groups [21].

3.2. *Effect of initial pH on Co(II), Cu(II), Ni(II), and Cd(II) ion adsorption and the zeta potential*

The effect of pH plays an important role on the active sites of bio-adsorbent as well as the heavy metal speciation during the adsorption reaction. In order to evaluate the influence of pH on the adsorption capacity of the barley straw ash, experiments were carried out at initial concentration of 10.5 mg/L and in the pH range 1.0–12.0 (Fig. 3A).

Fig. 3A shows the varying Co(II), Cu(II), Ni(II), and Cd(II) ions uptake capacity on the ash, at various pH values. The observed lower uptake in an acidic medium may be due to particle attrition, partial protonation of the functional groups and the competition between H+ and metal ions for binding to the adsorption sites of the ash (the active sites are closely associated with hydronium ions H_3O^+, that

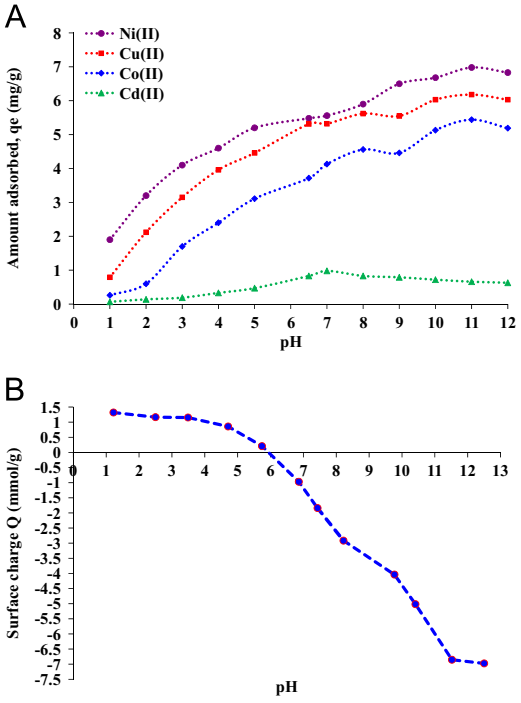

Fig. 3. (A) Effect of pH on the heavy metals ions sorption from aqueous solution by barley straw ash, (B) Zeta potential of the barley straw ash as a function of pH ($C_{biomaterial}$=2.5 g $L^{-1}$and 10^{-3} mol L^{-1} solution of KNO_3). Experimental error: ±4 mV.

is, restricted the approach of heavy metals as a result of the repulsive force). Thus, removal of heavy metals increases with increasing solution pH, reaching a maximum value at an optimal equilibrium pH of around 11.0.

The Cd(II) sorption capacity of the ash increased steadily with increase in pH up to 7.0, after which it decreased whereas the removal capacity of Cu(II), Ni(II), and Co(II) on the ash increased constantly with increasing pH, and then increased slowly between pH of 7.0 and 12.0, reaching the highest level at pH above 10.0. The reduction in uptake rate at pH values higher than 11.0 may be explained to metal hydroxylation yielding metal hydroxides or hydrated oxides which leads to metal passivation [22,23]. However, by increasing pH (i.e., fewer H_3O^+, the surface active sites become more negatively charged), the adsorbent surface becomes deprotonated, resulting in more biomass active sites available for metal ion binding, and electrostatic attraction from free electron–pairs of –Si–OH, –P–OH and –Ca–OH groups are likely enhanced. Therefore, more active functional groups take part on metal ion uptake by complexation reaction or chelating and adsorbed amount consequently increases.

Consequently, the prepared biomass appears to be effective for the removal of heavy metal ions in a wide range of pH from 1.0 to 12.0, which might be promising in wastewater treatment. Therefore, removal of heavy metal ions increase with increasing solution pH and the maximum value was reached at an optimal equilibrium pH of around 7.0.

In order to a better comprehending of the net charge of the adsorbent surface at the different pH solutions, the point of zero charge (pH_{ZPC}; ZPC is defined as the pH at which the total surface charges become zero) of the BSA was measured. The results of pH_{ZPC} determination are shown in Fig. 3B. The BSA indicates a pH_{ZPC} of 5.95 which confirms that the surface of the BSA has negative charge in most of the investigated pHs (Fig. 3B).

3.3. Biosorption time of Ni(II), Cu(II), Co(II) and Cd(II)

The importance of stirring time comes from the need for characterization of the feasible rapidness of binding and removal processes of the used heavy metal ions by the newly bioadsorbent and obtaining the optimum time for complete removal of the target metal ions. The analysis of batch adsorption of metal ions was carried out in 5 min steps and the concentration of each sample was measured by atomic absorption spectroscopy after 90 min contact time. Therefore, the small aliquots of samples were withdrawn from the reaction flask at different time intervals with a HPLC syringe. The contents were centrifuged to separate the adsorbent and the liquid layer was analyzed. The data for adsorption experiment were replicated three times and the results were averaged. The standard deviation was less than 3.8%. Thus, the effect of shaking time (0–90 min) on the adsorption of Ni(II), Cu(II), Co(II) and Cd(II) (10.0 mg/L) by BSA (0.15 g), at 25 °C, in the solution with pH 6.5, is shown in Fig. 6A, from which it can be seen that the amount of adsorption increases with increasing contact time. Studies of the adsorption kinetics of the heavy metals removal revealed that the majority of metal ions were removed within the first 50 min of contact with the bioadsorbent. The removal of used heavy metals from solution completed within 90 min. The percentage of maximum adsorption was 60.0% for Ni(II) at 45 min. This initial rapid adsorption gives way to a very slow approach to equilibrium. Indeed, the fast adsorption during the initial stages is probably due to the high concentration gradient between the adsorbate in the solution and that on the adsorbent as there are a high number of vacant sites available during this period, while the obtained plateau after 50 min relates to a slow rate of adsorption which could be due to agglomeration of the heavy metal ions molecules on the ash of barley straw active sites [24]. Therefore, in order to optimize the adsorption process, the adsorption isotherms for the remaining initial concentrations were obtained for a time of 50 min.

3.4. Effect of the initial concentration on the uptake

The results obtained for the bioadsorbent upon varying the initial heavy metal ions concentrations (0.5–16 mg/L) is illustrated in Fig. 4, where the initial heavy metal ions concentration were increased, at 25 °C for 45 min. The increase in the loading capacity of sorbent with increasing heavy metal concentrations is due to the interaction between metal ions and bioadsorbent which provides the vital driving force to defeat the resistances to the mass transfer of metal ions between the aqueous

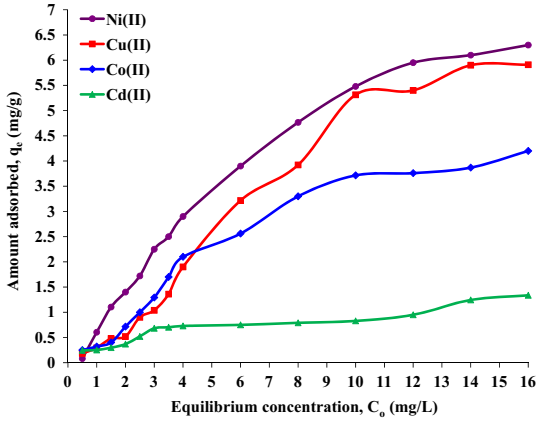

Fig. 4. Adsorption isotherms for the heavy metals adsorption over barley straw ash.

Table 1
Selected properties of the heavy metal ions.

Metal ions	Ionic radius (Å)	Hydrated ionic radius (Å)	Pauling's electronegativity
Cd(II)	0.95	4.26	1.69
Ni(II)	0.71	4.04	1.91
Cu(II)	0.73	4.19	1.90
Co(II)	0.74	4.23	1.88

and the bioadsorbent [25,26]. However, the observed increasing of the metal uptake with increasing initial metal ions concentration by the bioadsorbent could be due to an increase in electrostatic interactions (physical adsorption relative to covalent interactions), which involves active sites of progressively lower affinity for the heavy metal ions up to saturation point.

Despite the same experimental conditions used, it is interesting to note that the fixation capacities were also different according to the metal sorbed. The relative abilities of the solution species to compete for surface sites of the BSA are governed by intrinsic factors such as valence, ionic radius, pH, and the solution activities. Because the pH of the solution was kept constant and all the used heavy metals are divalent cations, the selectivity depends entirely on the hydrated radii of the ions. Lower binding capacity of Cd(II) ions over the other used metals ion on the biomass could be explained by the comparing the hydration radius and Pauling's electronegativity of Cd(II) ions with the other ones. Generally, at the same experimental conditions, the adsorption data show an affinity of the BSA for Ni (II) ion, which was confirmed by the steady state experiment (Fig. 4). The removal of heavy metals in this study were in the order of Ni(II) > Cu(II) > Co(II) > Cd(II), which coincide reasonably well with the reversed order trend of hydrated radius as Cd(II) (4.26 Å) > Co(II) (4.23 Å) > Cu(II) (4.19 Å) > Ni(II) (4.04 Å) and Pauling's electronegativity (Ni(II) (1.91) > Cu(II) (1.90) > Co(II) (1.88) > Cd(II) (1.69)) [27,28].

Due to the isotherm of Ni(II) adsorption and of Mg(II) desorption were practically similar (see Section 3.7), Ni(II) ions seemed to be exclusively adsorbed by an ion exchange mechanism. The smaller the ionic radius and the greater the valence, the more closely and strongly is the heavy metal ions adsorbed, thereby, the greater ion's hydration, the farther it is from the hydroxide surface and the weaker its removal. From the data of Table 1, the hydration radius of Ni(II) was the smallest, it exchanges easily with Mg(II) by ion exchange, so its removal was the highest. Likewise, the hydration radius of Cd(II) was the biggest, was the bigger than that of Mg(II) (ionic radius of Mg(II) is 0.72 Å), and it was difficult to react by ion exchange, so its removal was the lower.

Table 2
Fitting of the parameters of the experimental results to the Langmuir, Freundlich and Langmuir–Freundlich equation parameters.

Barley straw ash	q_e	K_L	K_F	n	R^2	χ^2	Sorption model
Cu(II)	17.8	5.92×10^{-2}			0.914	8.01	Langmuir
			1.19	7.09×10^{-1}	0.865	18.5	Freundlich
	6.04	3.71×10^{-2}		3.25×10^{-1}	0.993	0.003	Langmuir–Freundlich
Ni(II)	8.25	3.94×10^{-1}			0.977	0.464	Langmuir
			4.30	6.32×10^{-1}	0.808	0.930	Freundlich
	6.61	5.58×10^{-1}		6.85×10^{-1}	0.979	0.015	Langmuir–Freundlich
Co(II)	6.58	1.66×10^{-1}			0.955	0.860	Langmuir
			1.99	3.56×10^{-1}	0.834	2.44	Freundlich
	4.15	1.63×10^{-1}		4.82×10^{-1}	0.988	0.006	Langmuir–Freundlich
Cd(II)	1.42	2.73×10^{-1}			0.867	0.045	Langmuir
			1.41	6.60×10^{-1}	0.874	0.004	Freundlich
	74.2	4.94×10^{-3}		2.20	0.911	71.6	Langmuir–Freundlich

The inorganic pollutant adsorption isotherms can be classified within type S of the Giles adsorption isotherms classification [29,30]. The shape of the isotherms means that there is high affinity of the sorbent for low concentrations of metals in solution, where, the energy of activation for removal of metals from bioadsorbent is concentration-dependent and “cooperative adsorption” occurs, because in cooperative adsorption, sites capable of retaining a solute molecule increase.

3.5. Adsorption isotherms

The equilibrium adsorption isotherms are known one of the most important data to understand the mechanism of the adsorption and describe how adsorbate could interact with adsorbent. The experimental adsorption equilibrium data of heavy metals on BSA were fitted by applying the Langmuir, Freundlich and Langmuir–Freundlich isotherm models, which are usual models for the aqueous-phase adsorption (Table 2) [31]. These adsorption models give a representation of the adsorption equilibrium between an adsorbate in solution and the surface active sites of the adsorbent. The Langmuir, Freundlich and Langmuir–Freundlich adsorption isotherms can be expressed by the following equations:

$$q_e = q_m K_L C_e / 1 + K_L C_e \tag{2}$$

$$q_e = K_F {C_e}^{1/n} \tag{3}$$

$$q_e = q_m K_L {C_e}^{1/n} / 1 + K_L {C_e}^{1/n} \tag{4}$$

where q_e (mg/g) is the specific equilibrium amount of adsorbate, C_e (mg/L) is the equilibrium concentration of adsorbate, q_m (mg/g) is the maximal adsorption capacity and K (K_L and K_F) (L/mg) and n are empirical constants that indicate the extent of adsorption and the adsorption effectiveness, respectively. The constant n gives an idea of the grade of heterogeneity in the distribution of energetic centers and is related to the magnitude of the adsorption driving force [32]. High n values therefore indicate a relatively uniform surface, whereas low values mean high adsorption at low solution concentrations. Furthermore, low n values indicate the existence of a high proportion of high-energy active sites.

The Langmuir equation relates the coverage of molecules on the solid surface to concentration of a medium above the solid surface at a fixed temperature and adsorption is limited to monolayer coverage, and intermolecular forces decrease with the distance from the adsorption surface. On the other hand, the Freundlich model supposes that the adsorption surface is heterogeneous, that interactions among adsorbed molecules can occur, and that multilayer adsorption is possible. The Langmuir, Freundlich and Langmuir–Freundlich adsorption isotherms exhibit an approximately linear

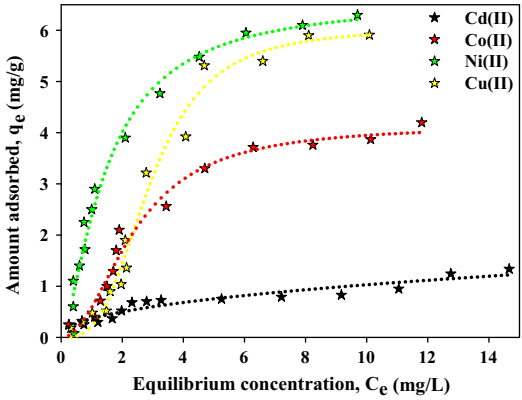

Fig. 5. Equilibrium absorption of the heavy metals by the BSA at 25 °C and pH = 6.5. Dash lines represent the fitting curve using the Langmuir–Freundlich adsorption model.

relationship for barley straw ash. The data obtained from the bioadsorbent revealed that the Langmuir and a combination of the Langmuir and Freundlich (L–F) isotherm models fitted the experimental data better ($R^2 > 0.911$) than the Freundlich isotherm (Fig. 5).

Furthermore, in order to determine the best isotherm that could describe adsorption process of the heavy metal ions, data analysis was performed using linear regression that fitness of the models is often evaluated based on the value of the correlation coefficients (R^2). But, the Langmuir and Langmuir–Freundlich isotherms give very high and close R^2 values that conclusion is not easy. Due to the resulting correlation coefficients (R^2) of the isotherms that were very close and high, Chi-square test is used to determine best isotherm models. Chi-square analysis has the advantage that all isotherms were compared on the same abscissa and ordinate which could be used to determine the best fitted model for isotherm. The Chi-square statistic test (Eq. (5)) is basically the sum of the squares of the differences between the experimental data and theoretically predicted data from models.

The Chi-square value is given as [33–35]:

$$\chi^2 = \sum_{i=1}^{i=N} \frac{(q_{e-} q_{em})^2}{q_{em}} \tag{5}$$

where q_{em} equilibrium capacity obtained by calculated from model (mg/g) and q_e was the equilibrium capacity (mg/g) from the experimental data. If data from the model were similar to the experimental data, χ^2 would be a small value and vice versa. Therefore, it is necessary to also analyze the data set using the Chi-square test to confirm the best fit isotherm for the sorption system. The values of χ^2 of each model were shown in Table 2. The Langmuir–Freundlich isotherm has the lowest χ^2 values for Ni (II), Cu(II), and Co(II), suggesting that the Langmuir–Freundlich isotherm provides the best fit to the experimental data. Therefore, it is realistic to infer that the adsorption active sites on the BSA are energetically heterogeneous (non-uniform surface) [36], and this is a major aspect in this model. However, in the case of Cd(II), the χ^2 value of the Freundlich isotherm has lower than the χ^2 values of Langmuir and Langmuir–Freundlich isotherms. In this study, we would like to point out that it is not appropriate to use the correlation coefficient (R^2) of linear regression analysis for comparing the best-fitting of Freundlich, Langmuir and Langmuir–Freundlich isotherms. Chi-square analysis would be a better criterion for avoiding such errors.

3.6. Kinetics study

In order to determine and interpret the mechanisms of heavy metal ions adsorption processes over the BSA and major parameters governing sorption kinetics, kinetic sorption data obtained empirically were fitted to the pseudo-first-order, pseudo-second-order, and intra-particle diffusion models shown as Eqs. (6)–(8). Each of which has been widely used to describe metal and organic sorption on different

sorbents [37,38]. From the linear form of these three models, equations can be written as follows:

$$\text{Pseudo}-\text{first}-\text{order equation}: \quad q_t = q_e[1-exp(-k_1 t)] \tag{6}$$

$$\text{Pseudo}-\text{second}-\text{order equation}: \quad q_t = k_2 q_e^2 t/1+k_2 q_e t \tag{7}$$

$$\text{Intra}-\text{particle diffusion equation}: \quad q_t = k_{int} t^{1/2} \tag{8}$$

The initial adsorption rate (h) can be determined from k_2 and q_e values using

$$h = k_2 q_e^2 \tag{9}$$

where k_1, k_2 and k_{int} are the adsorption rate constants of the first, the second-order kinetic and intra-particle diffusion models, in 1/min, g/(mg min) and mg/(g $\text{min}^{1/2}$), respectively; q_e and q_t in mg/g, are equilibrium adsorption uptake (at time $t=\infty$) and adsorption uptake (at time t), respectively.

The calculated kinetics parameters for adsorption of heavy metal ions onto the barley straw ash, at initial concentration of 10.0 mg/g are tabulated in Table 3. As can be observed, the pseudo-second-order equation appeared to be the best-fitting model than those for the other two equations (the correlation coefficient is extremely high for the pseudo-second-order equation of the barley straw ash; $R^2 > 0.978$). The plot of linear form of the pseudo-second-order for the adsorption of Ni(II), Cu(II), Co(II), and Cd(II) ions was shown in the inset of Fig. 6B. Similar results have been reported about the adsorption of heavy metals onto the different adsorbents in the literature [25,39].

The pact of the experimental data with the pseudo-second-order kinetic model (the pseudo-second-order equation is based on the sorption capacity on the solid phase) indicates that the adsorption of the metals ions onto the BSA controlled by chemisorption (as the rate-limiting step of the adsorption mechanism and no involvement of a mass transfer in solution) involving valence forces through sharing or exchange electrons between adsorbent and adsorbate [25,39–42]. As a result, the adsorption of the metals onto the bioadsorbent may be considered to composed of two processes with initial adsorption rate of 0.159, 0.167, 0.225, and 0.927 mg/(g min) for Ni(II), Cu(II), Co(II), and Cd(II), respectively, over BSA (the adsorption rate was related to the content and type of active adsorption site on the matrix of adsorbent).

Table 3
Kinetic parameters for the adsorption of heavy metals by barley straw ash.

System	First-order model			
	$k_1(\frac{1}{\text{min}})$		q_1 (mg/g)	R^2
Cu(II)	5.801		6.211	0.997
Cd(II)	13.37		0.974	0.938
Ni(II)	3.260		6.211	0.986
Co(II)	7.244		4.366	0.979
System	Second-order model			
	k_2 (mg/(g min))	q_2 (mg/g)	h (mg/(g min))	R^2
Cu(II)	0.167	5.988	1.483	0.997
Cd(II)	0.927	1.078	0.606	0.978
Ni(II)	0.159	6.289	1.730	0.999
Co(II)	0.225	4.444	0.561	0.9998
System		Inter-particle model		
		K_{int} (mg/(g $\text{min}^{1/2}$))		R^2
Cu(II)		0.128		0.780
Cd(II)		9.974		0.892
Ni(II)		3.107		0.826
Co(II)		2.980		0.865

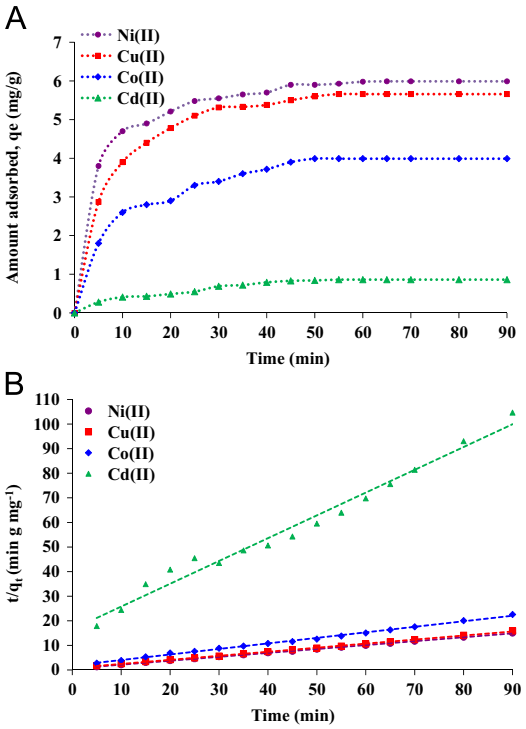

Fig. 6. The adsorption kinetics of the BSA for heavy metals at room temperature (A), plots of pseudo-second-order kinetics of the heavy metals adsorption (B).

3.7. *Effect of the temperature on the uptake of heavy metals*

The plot of adsorption vs. the final concentration of Ni(II), Cu(II), Co(II) and Cd(II) at varying range of temperature of solution shows that the adsorption of metals increases with increasing temperature in the solution (Fig. 7). This may indicate that adsorption of the heavy metals onto the active sites of bioadsorbent are endothermic and could be elucidated by availability of more active sites of adsorbent, the enlargement and activation of the adsorbent surface at higher temperatures. This could also be due to the easily mobility of heavy metals ions from the bulk solution towards the adsorbent surface and enhanced the accessibility to the adsorbent active sites.

In order to better understand the effect of rising temperature on the adsorption of the Ni(II), Cu(II), Co(II) and Cd(II) ions onto the barley straw ash, three basic thermodynamic parameters were studied: the Gibbs free energy of adsorption (ΔG°), the enthalpy change (ΔH°), and the entropy change (ΔS°).

The thermodynamic parameters ΔG°, ΔS° and ΔH° for this adsorption process were determined by using following equations.

$$\Delta G^\circ = -\mathrm{RT}\ \ln K \tag{10}$$

where K is the thermodynamic equilibrium constant. The values of K can be determined by plotting $\ln(q_e/C_e)$ against q_e and extrapolating to zero, where q_e is the adsorbed heavy metals ions concentration at equilibrium and C_e is the equilibrium concentration of heavy metals ions in solution. The effect of temperature on thermodynamic constant is determined by Eq. (11)

$$\mathrm{d}\ln K/\mathrm{d}t = \Delta H^\circ/\mathrm{RT}^2 \tag{11}$$

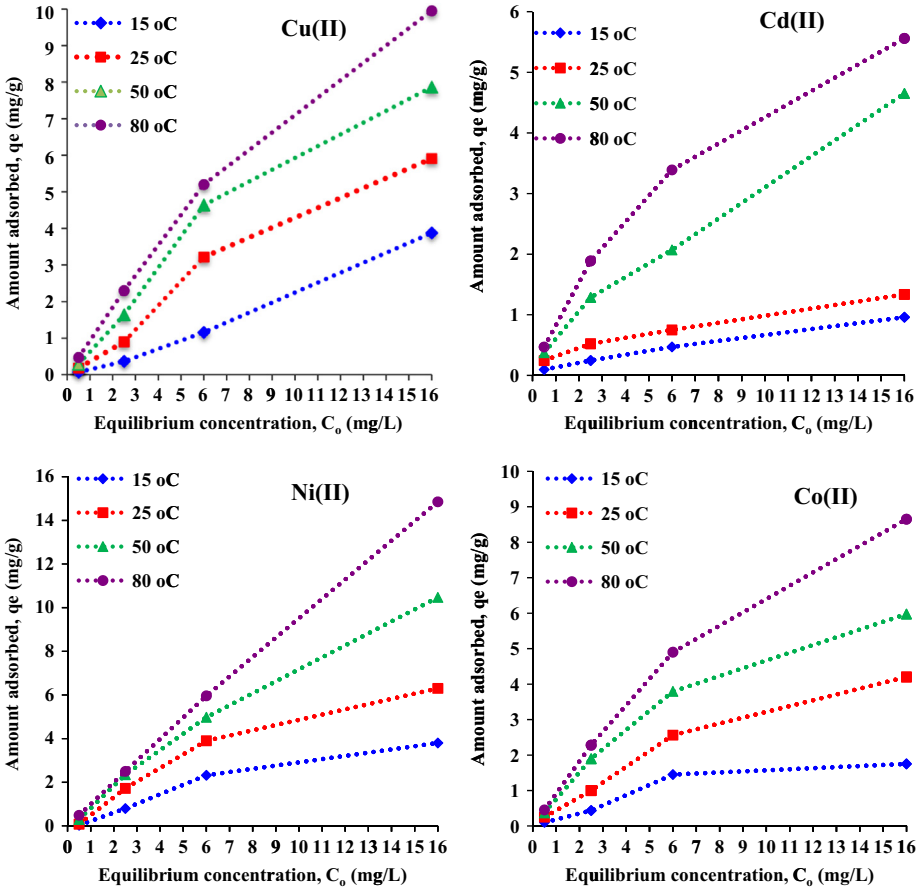

Fig. 7. Effect of temperature on the adsorption of the heavy metals by BSA at different initial concentrations.

The ΔH° and ΔS° values were calculated from slope and intercept of the linear plot, of ln K vs 1/T as shown in Figs. 8 and 9.

$$\ln K = \Delta S^\circ/R - \Delta H^\circ/RT \tag{12}$$

and the Gibbs free energy is given by Eq. (13), where ΔG° is the free energy change (J/mol); R and T is the universal constant (8.314 J/mol K) the absolute temperature (K), respectively.

$$\Delta G^\circ = \Delta H^\circ - T\Delta S^\circ \tag{13}$$

The corresponding values of thermodynamic parameters are presented in Table 4. This shows that ΔH^o and ΔS^o are positive for all the experiments and ΔG^o is negative in all systems. The positive values of ΔH^o revealed that the adsorption process was endothermic in nature; hence with increasing temperature the adsorbed amount at equilibrium increased. The positive value of ΔS° revealed the increased randomness and an increase in the degrees of freedom at the bioadsorbent-solution interface during the immobilization of the heavy metals ions on the active sites of the adsorbent, which indicate the partial liberation of the solvation metal ions from solvent molecules before adsorption (liberation of water molecules from solvated-heavy metals), therefore, enabling commonness of randomness and spontaneity in the system [43,44]. The necessity of a large amount of heat to remove the metals ions from the solution makes the sorption process endothermic.

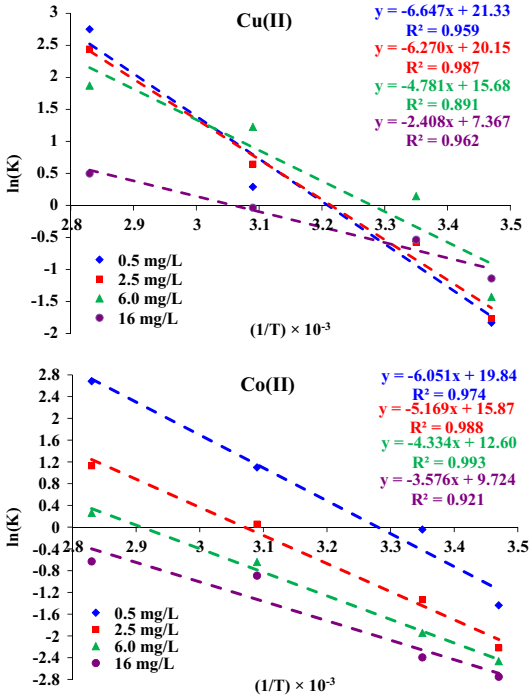

Fig. 8. Plots of ln K vs. 1/T for the Cu(II) and Co(II) adsorption on the barley straw ash.

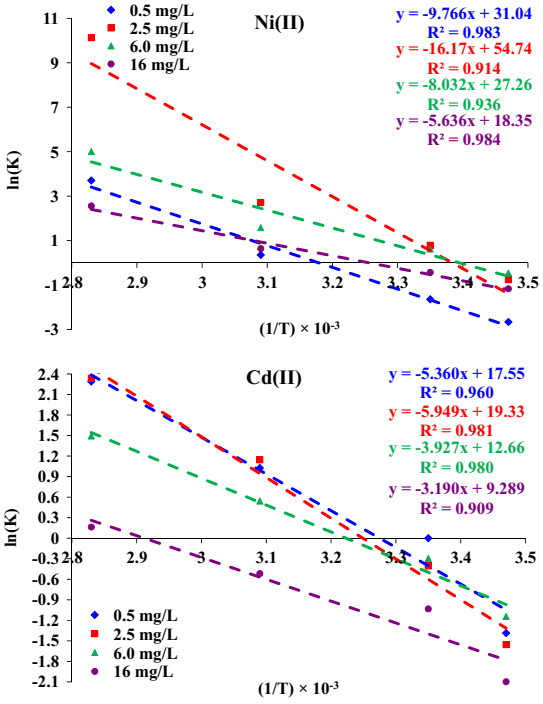

Fig. 9. Plots of ln K vs. 1/T for the Ni(II) and Cd(II) adsorption on the barley straw ash.

Table 4
Thermodynamic parameters for the adsorption of heavy metals onto BSA as a function of temperature.

Initial M(II) ions concn.	ΔH°	ΔS°	ΔG° (kJ/mol)			
mg/L	(kJ/mol)	(kJ/(mol K))	288	298	312	353
Cu(II)						
0.5	0.0553	0.1773	-51.00	−52.78	−55.26	−62.53
2.5	0.0521	0.1675	−48.18	−49.86	−52.20	−59.07
6.0	0.0397	0.1304	−37.51	−38.81	−40.64	−45.99
16	0.0200	0.0612	−17.60	−18.21	−19.07	−21.58
Cd(II)						
0.5	0.0503	0.1649	−47.44	−49.08	−51.39	−58.15
2.5	0.0429	0.1319	−37.94	−39.26	−41.10	−46.51
6.0	0.0360	0.1047	−30.11	−31.16	−32.63	−36.92
16	0.0297	0.0808	−23.24	−24.04	−25.17	−28.49
Ni(II)						
0.5	0.0811	0.2580	−74.24	−76.82	−80.43	−91.01
2.5	0.1344	0.4551	−130.9	−135.4	−141.8	−160.5
6.0	0.0667	0.2266	−65.20	−67.46	−70.64	−79.93
16	0.0468	0.1525	−43.89	−45.41	−47.55	−53.80
Co(II)						
0.5	0.0445	0.1459	−41.97	−43.43	−45.47	−51.46
2.5	0.0494	0.1607	−46.23	−47.83	−50.08	−56.67
6.0	0.0326	0.1052	−30.27	−31.33	−32.80	−37.12
16	0.0265	0.0772	−22.21	−22.98	−24.06	−27.23

The positive ΔS° (disorder of the system) was observed on the barley straw ash, which indicates that the metal ions lose most of their water of solvation [45]. This is also supported by the positive value of ΔH° in metals sorption onto the barley straw ash. The positive value of the standard enthalpy change for the metal ions sorption indicates endodermic nature of adsorption. It was also observed that with increase in temperature the value of ΔG^o decreases, which indicated that sorption processes was spontaneous and thermodynamically favorable by an increase in temperature (Table 4).

3.8. Adsorption mechanisms

The adsorption study of heavy metals onto the BSA has highlighted an ion exchange mechanism responsible for metal uptake. The term “adsorption” usually describes the change in concentrations of chemical constituents in the solid phase as a result of mass transfer between solution and solid, and thus adsorption involves different types of removal mechanisms such as adsorption, absorption, and exchange [39]. To demonstrate the adsorption mechanism(s) for the removal of the used heavy metals in this research, a number of cations are analyzed in addition to target heavy metals in the solutions using ICP-AES.

Through the leaching experiments of the BSA using deionized water under condition equivalent to kinetic adsorption tests, it was demonstrated that the metal ions (Mg(II), K(I), and Ca(II)) were released at only very low levels of 0.65, 0.17, and 0.04 mg/L, respectively, after a reaction time of 24 h. The results show that the leaching of these cations from the BSA is very slow under the experimental condition. However, in the sorption experiments for heavy metals, Mg, K, and Ca concentrations gradually increased over the contact time. Concentrations increased up to 4.3, 1.9 and 0.35 mg/L for Mg(II), K(I) and Ca(II), respectively, and the sequence of concentrations was Mg (II) > K(I) > Ca (II) at each sampling event, which suggests that Ca(II), K(I), and Mg(II) ions were really neutralizing the moieties of the BSA before metal adsorption. The concentrations (meq/L) of the sorbed heavy metals versus the sum of concentrations of released cations (Ca(II)+K(I)+Mg(II)) within all the kinetic

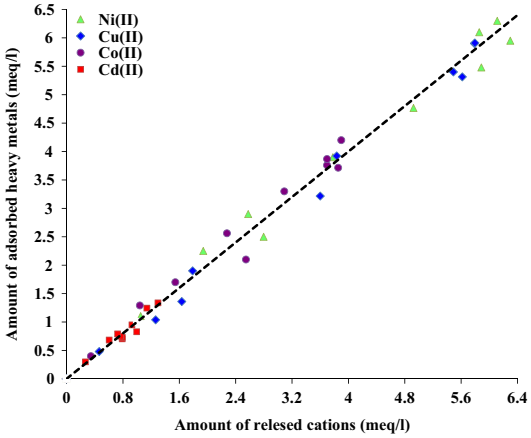

Fig. 10. Correlations between the concentrations (meq/l) of adsorbed heavy metals onto the BSA and the amount of concentrations of cations released into solution with a 1:1 correlation dash line. All data used were obtained from kinetic sorption tests onto the barley straw ash.

experiments is shown in Fig. 10. Because the isotherm of heavy metals adsorption and cations desorption were practically similar, heavy metal ions seemed to be exclusively adsorbed by an ion exchange mechanism which can be expressed by the following balanced equations [46]:

$$BMe + HM(s)^{2+} \leftrightarrow BHM(s) + Me^{(2)+} \tag{14}$$

$$\sum[Me^{(2)+}] = \sum\Delta[HM(s)^{(2)+}] \tag{15}$$

where Me and HM(s) represent weakly bound major cations (Mg(II), K(I), and Ca(II)) and sorbate metals (Ni(II), Cu(II), Co(II), Cd(II)), respectively, and [ ] denotes the concentration (meq/L) in the solution.

However, for each metal, the difference between the adsorption isotherm and the cations desorption isotherm could be related to the extent of a complexation/chelation mechanism completing the ion exchange one, where the extent of these mechanisms depended on the nature of the metal.

In addition, the carbon content was demonstrated to remove the radioactive ion [47]. Therefore, it is believed that the remained organic compounds were activated at high temperatures to develop basic oxides on the surface during the treatment process of bioadsorbent (barley straw ash), the lone pair of electrons associated with the oxygen atoms chemisorbed onto the surface and would be coordinated to the inner transition metal vacant d-orbitals to form a type coordination bond. But no conclusive evidence for this effect has been shown in this paper. However, we can conclude from the alkali cations-exchange mechanism that a part of metal ions uptake is due to the ion exchange process. The sorption mechanisms can be attributed to at least two pathways:

1. Ion exchange of divalent metal ions from the surface of barley straw ash.
2. Adsorption of metal ions from the carbon surface.

3.9. Reusability test

Elemental analysis indicated that only a trace amount of metal was released during this process 0.06% Ni(II) and 0.09% Cu(II) were released from the bioadsorbent. The regenerated biomaterial was treated with $Ni(NO_3)_2$ and $Cu(NO_3)_2$ solutions, which loading of 6.12 and 5.79 mg/g, respectively, were obtained, corresponding to about 98% of the original loading capacities. Similar results were obtained

for a third, fourth and fifth regenerations and reuse cycle. These results indicated that the novel bioadsorbent remains effective even after extended regeneration and reuse cycles.

4. Conclusions

The biosorption properties of BSA were studied for Ni(II), Cu(II), Co(II), and Cd(II) ions in the present work. The results show that the BSA may be used as an inexpensive, selective, effective and easily cultivable biosorbent that can be applied in water and wastewater treatment for the adsorption of metal species.

The operating parameters, pH of solution, contact time, and temperature, were effective on the removal efficiency of the heavy metals ion. The selectivity sequence of the adsorption edges of these metals were Ni(II) > Cu(II) > Co(II) > Cd(II). Equilibrium isotherms have been measured experimentally and analyzed by various equation isotherm models. The Langmuir–Freundlich isotherm equation was found to best represent the experimental adsorption data obtained in adsorption of heavy metal ions from aqueous solutions by the bioadsorbent. The calculated thermodynamic parameters indicated the feasibility, endothermic and spontaneous nature of the adsorption process. Kinetic studies showed that the adsorption of heavy metal ions on the bioadsorbent followed well the pseudo-second-order kinetic model. In order to realize its full potential as a commercial sorbent, uptake of metals under continuous condition with industrial wastewater containing such toxic metals must be evaluated. Currently such an investigation is being undertaken.

References

[1] R. Lal, World crop residues production and implications of its use as a biofuel, Environ. Int. 31 (2005) 575–584.
[2] S.V. Vassilev, D. Baxter, L.K. Andersen, C.G. Vassileva, An overview of the composition and application of biomass ash. Part 1. Phase–mineral and chemical composition and classification, Fuel 105 (2013) 40–76.
[3] C. Serrano, Esperanza Monedero, Magín Lapuerta, Henar Portero Agronomic Effect of moisture content, particle size and pine addition on quality parameters of straw barley straw pellets, Fuel Process. Technol. 92 (2011) 699–706.
[4] D. Nordgren, H. Hedman, N. Padban, D. Boström, M. Öhman, Ash transformations in pulverised fuel co-combustion of straw and woody biomass, Fuel Process. Technol. 105 (2013) 52–58.
[5] M. Han, K.E. Kang, Y. Kim, G.-W. Choi, High efficiency bioethanol production from straw barley straw using a continuous pretreatment reactor, Process Biochem. 48 (2013) 488–495.
[6] S.V. Vassilev, D. Baxter, L.K. Andersen, Christina G. Vassileva, Trevor J. Morgan, An overview of the organic and inorganic phase composition of biomass, Fuel 94 (2012) 1–33.
[7] B. Volesky, Detoxification of metal-bearing effluents: biosorption for the next century, Hydrometallurgy 59 (2001) 203–216.
[8] M. Arshadi, M. Ghiaci, A. Gil, Schiff base ligands immobilized on a nanosized SiO_2–Al_2O_3 mixed oxide as adsorbents for heavy metals, Ind. Eng. Chem. Res. 50 (2011) 13628–13635.
[9] L. Deng, X. Zhu, X. Wang, Y. Su, H. Su, Biosorption of copper(II) from aqueous solutions by green alga *Cladophora fascicularis*, Biodegradation 18 (2007) 393–402.
[10] C.H. Weng, C.P. Huang, Treatment of metal industrial wastewater by fly ash and cement fixation, J. Environ. Eng. 120 (1994) 1470–1487.
[11] V.K. Gupta, A. Rastogi, Sorption and desorption studies of chromium (VI) from nonviable cyanobacterium Nostoc muscorum biomass, J. Hazard. Mater. 154 (2008) 347–354.
[12] A. Saeed, M. Iqbal, M.W. Akhtar, Removal and recovery of lead (II) from single and multimetal (Cd, Cu, Ni, Zn) solutions by crop milling waste (black gram husk), J. Hazard. Mater. 117 (1) (2005) 65–73.
[13] G. Vazque, A.J. Gonzalez, A.L. Garcia, M.S. Freire, G. Antorrena, Adsorption of phenol on formaldehyde-pritreated Pinus pinaster bark: equilibrium and Kinetics, Bioresour. Technol. 98 (8) (2007) 1535–1540.
[14] B. Yu, Y. Zhang, A. Shukla, S. Shukla, K.L. Dorris, Removal of heavy metals from aqueous solution by sawdust adsorption of lead and comparison of its adsorption with copper, J. Hazard. Mater. 84 (1) (2001) 83–94.
[15] V. Vinodhini, N. Das, Relevant approach to assess the performance of sawdust as adsorbent of chromium (VI) ions from aqueous solutions, Int. J. Environ. Sci. Technol. 7 (1) (2010) 85–92.
[16] S.K. Wisniewska, J. Nalaskowski, E. Witka-Jezewska, J. Hupka, J.D. Miller, Surface properties of barley straw, Colloids Surf. B 29 (2003) 131–142.
[17] R. Cason, W.R. Lester, Chemistry of two clay systems and three phenoxy herbicides, Proc. Okla. Acad. Sci. 57 (1977) 116–118.
[18] E.T. Stathopoulou, V. Psycharis, G.D. Chryssikos, V. Gionis, G. Theodorou, Bone diagenesis: new data from infrared spectroscopy and X-ray diffraction, Palaeogeogr., Palaeoclimatol., Palaeoecol. 266 (2008) 168–174.
[19] T. Ishikawa, M. Wakamura, S. Kondo, Surface characterization of calcium hydroxylapatite by Fourier transform infrared spectroscopy, Langmuir 5 (1989) 140–144.
[20] E. Wojciechowska, A. Włochowicz, A. Wesełucha-Birczynskab, Application of Fourier-transform infrared and Raman spectroscopy to study degradation of the wool fiber keratin, J. Mol. Struct. 511–512 (1999) 307–318.
[21] T.Z. Ren, Z.Y. Yuan, B.L. Su, Surfactant-assisted preparation of hollow microspheres of mesoporous TiO_2, Chem. Phys. Lett. 374 (1–2) (2003) 170–175.

[22] Y. Xue, H. Hou, S. Zhu, Competitive adsorption of copper(II), cadmium(II), lead(II) and zinc(II) onto basic oxygen furnace slag, J. Hazard. Mater. 162 (2009) 391–401.
[23] Z. Aksu, D. Akpinar, Competitive biosorption of phenol and chromium(VI) from binary mixtures onto dried anaerobic activated sludge, Biochem. Eng. J. 7 (2001) 183–193.
[24] J. Achary, J.N. Sahu, C.R. Mohanty, B.C. Meikap, Removal of lead(II) from wastewater by activated carbon developed from Tamarind wood by zinc chloride activation, Chem. Eng. J. 149 (2009) 249–262.
[25] M. Ghiaci, M. Arshadi, M.E. Sedaghat, R.J. Kalbasi, A. Gil, Adsorption of organic pollutants from aqueous solutions on cereal ashes, J. Chem. Eng. Data 53 (2008) 2707–2709.
[26] M. Arshadi, F. Salimi Vahid, J.W.L. Salvacion, M. Soleymanzadeh, A practical organometallic decorated nano-size SiO_2–Al_2O_3 mixed-oxides for methyl orange removal from aqueous solution, Appl. Surf. Sci. 280 (2013) 726–736.
[27] D.R. Lide, Handbook of Chemistry and Physics, 79th ed., CRC Press, Boca Raton5–93.
[28] E.R. Nightingale, Phenomenological theory of ion solvation effective radii of hydrated ions, J. Phys. Chem. 63 (1959) 1381–1387.
[29] C.H. Giles, D. Smith, A. Huitson, A general treatment and classification of the solute adsorption isotherm, J. Colloid Interface Sci. 47 (1974) 755–765.
[30] C.H. Giles, T.H. McEvan, S.N. Nakhawa, S.D. Smith, Studies in adsorption Part XI. A system of classification of solution adsorption isotherms, and its use in diagnosis of adsorption mechanisms and in measurement of specific surface area of solid, J. Chem. Soc. 5 (1960) 3973–3993.
[31] D.D. Do, Adsorption Analysis: Equilibria and Kinetics, Imperial College Press, London, 1998.
[32] M. Yurdakoc, Y. Scki, S.K. Yuedakoc, Kinetic and thermodynamic studies of boron removal by Siral 5, Siral 40, and Srial 80, J. Colloid Interface Sci. 286 (2005) 440–446.
[33] T.K. Naiya, A.K. Bhattacharya, S.K. Das, Clarified sludge (basic oxygen furnace sludge)—an adsorbent for removal of Pb(II) from aqueous solutions—kinetics, thermodynamics and desorption studies, J. Hazard. Mater. 170 (2009) 252–262.
[34] Y.S. Ho, Selection of optimum sorption isotherm, Carbon 42 (2004) 2113–2130.
[35] A. Afkhami, M. S.-Tehrani, H. Bagheri, Simultaneous removal of heavy-metal ions in wastewater samples using nano-alumina modified with 2,4-dinitrophenylhydrazine, J. Hazard. Mater. 181 (2010) 836–844.
[36] Y. Mao, B.M. Fung, Formation and characterization of anchored polymer coatings on alumina, Chem. Mater. 10 (1998) 509–517.
[37] R.C. Bansal, Activated Carbon Adsorption, CRC Press, Boca Raton, FL, 2005.
[38] Y.S. Ho, G. McKay, The kinetics of sorption of divalent metal ions onto sphagnum moss peat, Water Res. 34 (2000) 735–742.
[39] J. Febriantoa, A.N. Kosasih, Jaka Sunarso, Yi-Hsu Ju, Nani Indraswati, Suryadi Ismadji, Equilibrium and kinetic studies in adsorption of heavy metals using biosorbent: a summary of recent studies, J. Hazard. Mater. 162 (2009) 616–645.
[40] P. Miretzky, C. Munoz, A. Carrillo-Chavez, Experimental binding of lead to a low cost on biosorbent: nopal (*Opuntia streptacantha*), Bioresour. Technol. 99 (2008) 1211–1217.
[41] X.Y. Guo, A.Z. Zhang, X.Q. Shan, Adsorption of metal ions on lignin, J. Hazard. Mater. 151 (2008) 134–142.
[42] K.C. Bhainsa, S.F. D'Souza, Removal of copper ions by the filamentous fungus,*Rhizopus oryzae* from aqueous solution, Bioresour. Technol. 99 (2008) 3829–3835.
[43] R. Han, W. Zou, Y. Wang, L. Zhu, Removal of uranium (VI) from aqueous solutions by manganese oxide coated zeolite: discussion of adsorption isotherms and pH effect, J. Environ. Radioact. 93 (2007) 127–143.
[44] A. Sari, D. Mendil, M. Tuzen, M. Soylak, Biosorption of palladium(II) from aqueous solution by moss (Racomitrium lanuginosum) biomass: equilibrium, kinetic and thermodynamic studies, J. Hazard. Mater. 162 (2009) 874–879.
[45] E. Tipping, Interactions of organic acids with inorganic and organic surfaces, in: E.M. Perdue, E.T. Gjessing (Eds.), Organic Acids in Aquatic Ecosystems. Life Sciences Research Reports, Wiley, New York 1990, pp. 209–221.
[46] J.-S. Kwon, S.-T. Yun, S.-O. Kim, B. Mayer, I. Hutcheon, Sorption of Zn(II) in aqueous solutions by scoria, Chemosphere 60 (2005) 1416–1426.
[47] M.W. Abdel Raouf, A.A.M. Daifullah, Potential use of bone charcoal in the removal of antimony and europium radioisotopes from radioactive wastes, Adsorpt. Sci. Technol. 15 (1997) 559–569.